

# Engineered chemistry of Cu–W composites sintered by field-assisted sintering technology for heat sink applications

A. Rape · S. Chanthapan · J. Singh ·  
A. Kulkarni

Received: 11 June 2010/Accepted: 14 August 2010/Published online: 3 September 2010  
© Springer Science+Business Media, LLC 2010

**Abstract** High performance microelectronics require superior thermal management systems. Heat sink plates that dissipate the heat generated by the microelectronic components are of critical importance for this purpose. The two primary concerns with heat sink materials are the coefficient of thermal expansion (CTE), which should be low to match that of silicon ( $4 \times 10^{-6}/^{\circ}\text{C}$ ), and the thermal conductivity, which should be as high as possible to move the heat efficiently. This study created copper–tungsten composite materials using the field assisted sintering technology (FAST) process. The amount of tungsten used in the composites was varied from 0 to 70 wt% to study the effects of tungsten as well as to show the ability of the composite's properties to be tailored based on the percentage of tungsten in the composite. It is shown that increasing pressure has a positive effect on final density while heating rate has no effect. High densities of >97.5% were achieved in all of the composites. As predicted, the CTE decreases as the percentage of tungsten increases. Thermal conductivities are also reported for each sample.

## Introduction

Thermal management is a critical issue in the development of high performance microelectronics such as computers, cell phones, and other electronics. Heat sink plates are used

to dissipate the heat generated by the integrated circuit (IC). As the size of the IC shrinks, the current density increases meaning more concentration of heat that needs to be dissipated. To compensate for increased current density, more efficient heat sink plates must be developed. The major issues that face the development and inclusion of heat sink plates into electronic packages are heat dissipation, thermal stressing issues, and warping. Poor heat sink performance can limit the performance and lifetime of the device.

The goal of the heat sink plate is to provide a large surface area to allow the heat to dissipate and reduce thermal stress of the package. In general, heat sinks are designed to transfer heat as efficiently as possible to the surroundings. Therefore, materials with high thermal conductivity, such as copper, are desired. However, most common (with the exception of diamond and some ceramic) materials with a high thermal conductivity (such as copper) also have a high coefficient of thermal expansion (CTE). This is in sharp contrast to the low CTE of chip materials such as Si, SiC, AlN, and Al<sub>2</sub>O<sub>3</sub> (Si has a CTE of  $4 \times 10^{-6}/^{\circ}\text{C}$ , thermal conductivity of  $\sim 100 \text{ W/m K}$  at room temperature), which are used for the basis of the electronic package. The mismatch of CTE leads to stress fracturing at the interface between the two materials [1]. One approach to solving this problem is to tailor the material of the heat sink to have more desirable properties by blending two or more different materials that have desirable properties. One combination is tungsten and copper composite. The use of tungsten–copper (W–Cu) materials has great potential in thermal management applications such as heat sinks due to the low coefficient of expansion (which is consistent with that of IC substrates) of tungsten and the high thermal conductivity of copper. However, due to the mutual insolubility of copper and

A. Rape · S. Chanthapan · J. Singh (✉)  
Applied Research Laboratory, Pennsylvania State University,  
University Park, PA, USA  
e-mail: jxs46@psu.edu

A. Kulkarni  
Department of Mechanical Engineering, Pennsylvania State  
University, University Park, PA, USA

tungsten in the solid state as well as the large difference in melting temperatures (3,410, 1,083 °C for W, Cu, respectively), it is difficult to form Cu–W composite using conventional sintering techniques.

The most common route to produce W–Cu composites is to squeeze liquid copper to a pre-sintered porous tungsten structure under pressure. This is known as the infiltration process. This is undesirable because of high production costs and long-lead time. In the case of pure liquid phase sintering (without using a pre-sintered W structure), the low contact angle between the Cu and W particles gives rise to particle rearrangement. Densification is then completed by capillary forces exerted by the liquid. However, this requires the minimum amount of liquid copper to be 30 wt% [2–4].

Several works have been done previously in the area of Cu–W composites using related technologies. Cu–W composites with 50 and 75 wt% Cu were sintered to 98.6 and 98.5% of theoretical density, respectively, using the pulse plasma sintering technique at 900 °C. These composites showed strong influence of the W on the composite's CTE which ranged from 7 to  $15 \times 10^{-6}/\text{°C}$  [5]. Another study has been done that examine properties of Cu–W systems with 85 wt% W using FAST [6]. This study is fundamentally different because sintering temperatures ranging from 1,230 to 1,300 °C were used. Since this temperature range is well above melting temperature of copper, this indicates that the conventional liquid phase sintering mechanisms described above are responsible for densification [6]. In other systems, heating rate has been shown to have an effect on the final density in other material systems such as alumina [7], but not in nanocrystalline copper [8].

An alternative method has been done in which tungsten trioxide ( $\text{WO}_3$ ) and cupric oxide ( $\text{CuO}$ ) were mixed in a

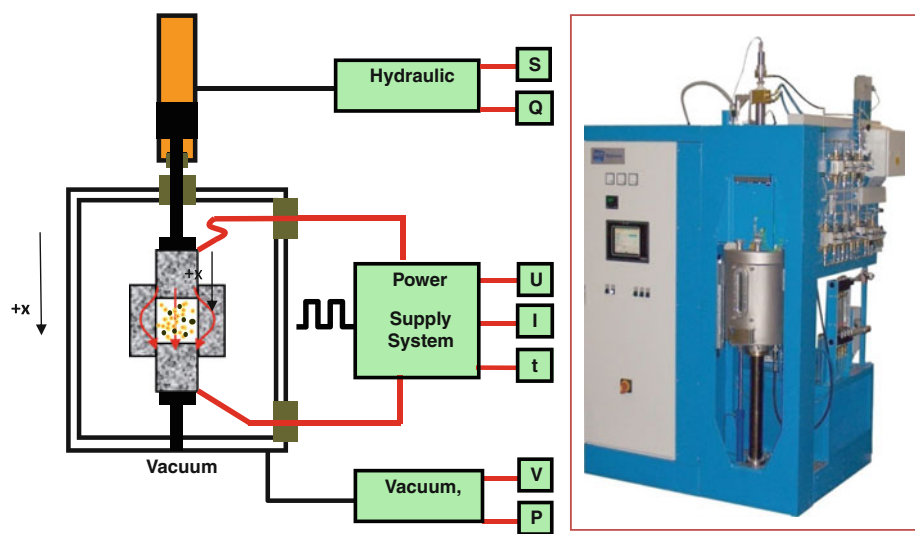
ball mill and then reduced in a hydrogen atmosphere to achieve a Cu–W composite powder as a starting point. Unlike liquid phase sintering, this method allows for the any desired ratio of Cu and W to be used. The method of reducing oxides exhibited higher densities up to 98% in the 80% W sintered samples. However, the downside to this process is that it is a multi-step process that requires longer time [9].

Powder metallurgy will be explored to meet the goal of high density, low CTE, highly thermally conductive material that is suitable for heat sink applications. In this work, the FAST process was used to densify a full range of Cu–W composites with varying amounts of Cu. Cu–WC composites were also studied because the composite material would be predicted to have similar properties to the Cu–W system except have a lower thermal conductivity due to WC having a lower thermal conductivity than W. Elemental powders were mechanically alloyed before being compacted. Process parameters such as temperature, pressure, and heating rate were investigated to determine optimal settings for maximum densification. The samples were evaluated for microstructure, thermal conductivity, and CTE.

### Field assisted sintering technology

FAST is a relatively new sintering technique that utilizes the simultaneous application of high temperature, uniaxial pressure, and DC current. A schematic of the FAST system is shown in Fig. 1. A very high, pulsed electric current allows for an extremely fast heating rate, which is combined with the pressure, results in the rapid densification of powders [10]. The powder to be sintered is placed inside a graphite die between two graphite punches. The punches

**Fig. 1** Schematic diagram of FCT FAST system



and die are separated from the powder with graphite foil. This prevents reaction with the graphite die at the temperatures used in this study. Pressure is applied to the punches and current is passed through them, as well as the die. The current through the die provides radiant heat to the powder. Current can also flow through the powder which causes Joule heating instantly. The current flows through the powder along the contact points between the particles (which become the grain boundaries) because it is the path of least resistance. Any resistance between current paths can cause fast heating and lead to melting, vaporization, and/or plasma formation. Under pressure, the particles rearrange and deform resulting in mechanical bonding as well as solid state joining through grain boundary diffusion. When the pressure is combined with high temperatures, the sintering rate is significantly improved. This process has the advantage over other methods of having significantly shorter sintering times and lower sintering temperatures [11].

## Experimental procedure

Elemental W (0.6–0.9  $\mu\text{m}$ ) or WC (1.2  $\mu\text{m}$ ) and Cu (43  $\mu\text{m}$ ) powder were weighed into a Nalgene bottle to the predetermined composition percentages and placed in a three-dimensional mixer to distribute the powders. Tungsten balls were added as the milling media at a ratio of roughly 5:1 (balls: powder). The bottle was filled with Ar and placed on rollers (KB Penta Power Model 4000, Chagrin Falls, OH) at a speed of 250 rpm and left for 20 h.

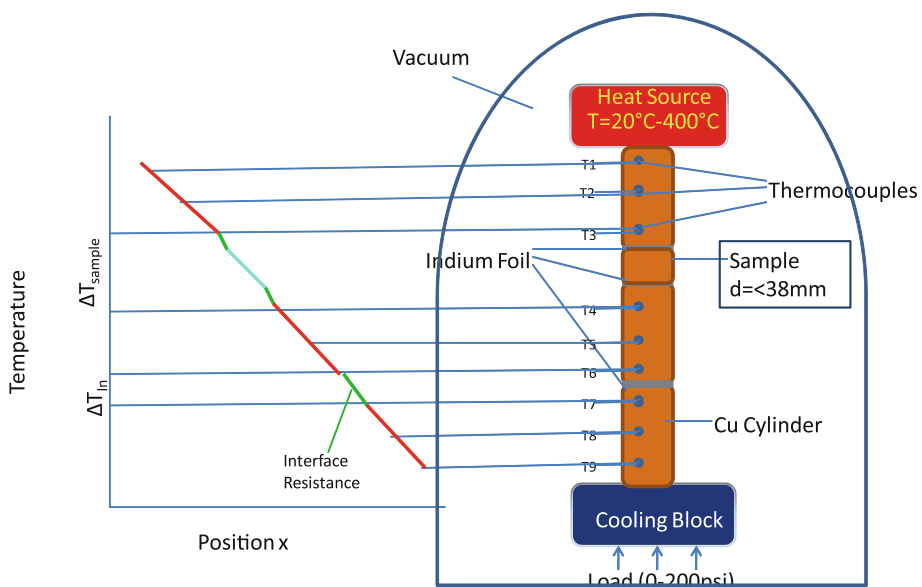
The alloyed powder was then compacted into a 40-mm diameter cylindrical graphite die lined with graphite foil. The die was placed into the FAST unit (FCT, Germany) for

densification. All powders underwent a reduction process in the FAST unit under an H<sub>2</sub> environment ranging in time from 20 min to an hour at 700 °C to remove any possible oxide that may have formed on the copper. Temperature and pressure were varied between runs to determine optimal parameters for maximum densification.

Sample densities were measured using the Archimedes method. Samples were then cut with a diamond saw and ground with SiC paper to 800 grit. The samples were then wet-polished using diamond suspensions down to 0.04  $\mu\text{m}$ . Optical and scanning electron microscopes were used to characterize the microstructure of sintered samples. CTE measurements were taken on a small section of the sample (roughly 5 × 5 mm) in the range of 5–250 °C using a TMA 2950 from TA Instruments.

The thermal conductivity was measured using a steady state comparative longitudinal heat flow for different thickness (SCHF-DT) method [12]. Figure 2 shows a schematic of the system used to measure the thermal conductivity of the thin samples. The sample dimensions for thermal conductivity can range from roughly 1 to 10 mm in thickness and 10–38 mm diameter. The samples used in this study were cut to 18 mm using wire EDM. This method uses three identical cylindrical Cu rods with three small holes drilled for thermocouples. The ends of the rods are sanded and cleaned with alcohol to ensure smooth, equivalent surface contact for each interface. The rods are stacked linearly along with the sample with indium foil at each interface to further ensure good thermal contact. The stack is then subjected to a load of 100 psi. Heat is provided to the top of the stack with an electric heater and cooling water is passed through the bottom to provide a temperature gradient across the stack as shown in Fig. 2. The system is placed under vacuum and heated until steady

**Fig. 2** Schematic diagram of thermal conductivity system



state is reached. Once steady state is reached, temperatures are recorded for each of the thermocouple positions. The heat flux through each of the bars is calculated by [12]:

$$q_1 = k_{\text{Cu}} \left( \frac{dT_1}{dx_1} \right), \quad (1)$$

where  $q_1$  is the heat flux through the top Cu rod,  $k_{\text{Cu}}$  is the thermal conductivity of copper, and  $(dT_1/dx_1)$  is the temperature gradient between the top and bottom thermocouple. The heat flux through the sample was estimated by averaging the heat flux through each of the rods:

$$q = \frac{q_1 + q_2 + q_3}{3} \quad (2)$$

The thermal resistance between any two thermocouples ( $i, j$ ) is given by:

$$R_t = \frac{\Delta T_{ij}}{qA_s}, \quad (3)$$

where  $\Delta T_{ij}$  is the temperature difference between any two thermocouples,  $q$  is the heat flux defined above, and  $A_s$  is the cross-sectional area of the sample. The thermal resistance can be attributed to the copper between the end of the thermocouple ( $R_{\text{Cu}}$ ), the interface between the rods ( $R_{\text{interface}}$ ), and the sample ( $R_{\text{sample}}$ ). Hence,

$$R_t = R_{\text{Cu}} + R_{\text{interface}} + R_{\text{sample}} \quad (4)$$

An in situ calculation of the thermal resistance is done on the bottom interface between the two copper rods. It is assumed that this thermal resistance is the same as each of the thermal resistances between the interfaces between the sample and copper rods. The thermal resistance of the sample is given by:

$$R_s = \frac{x_s}{K_{\text{sample}} A_s}, \quad (5)$$

where  $k_{\text{sample}}$  is the thermal conductivity of the sample. Substituting (3) and (5) into (4) and rearranging gives an expression for the thermal conductivity for the unknown sample [12]. This method is used to determine the thermal resistance rather than Eq. 5 because the thermal conductivity of the sample is unknown and cannot be incorporated into the equation.

$$k_s = \frac{x_s}{A_s(R_t - R_{\text{Cu}} - 2R_{\text{int}})} \quad (6)$$

## Results and discussion

Figure 3 shows the maximum densities accomplished for the Cu–W system with 10, 22, 50, and 70 wt% W. The trend is that the density is decreasing with increasing percentage of tungsten. Densities of at least 99% were achieved in each of the different tungsten compositions

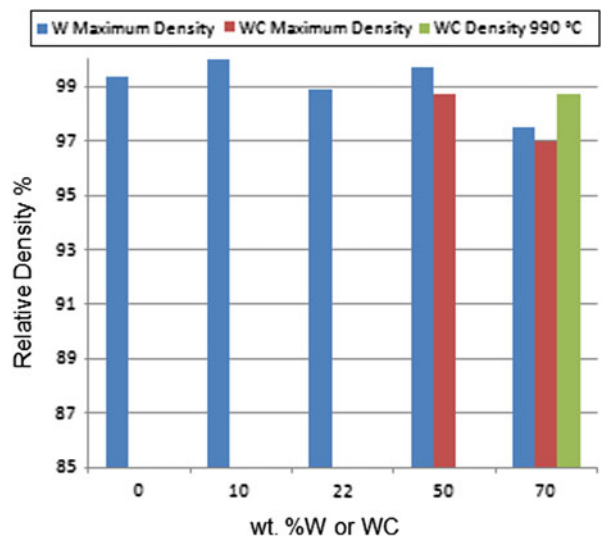


**Fig. 3** Maximum density achieved for the range of W–Cu compositions at sintering temperature of 975 °C for 20 min with pressures ranging from 36 to 75 MPa. The exception is the Cu–70 wt% WC sample sintered at 975 °C that showed an increase in final density when sintered at 990 °C

except for 70 wt% W. This is most likely due to the fact that the sintering temperature used in these experiments (975 °C) are very low compared to the temperature that pure tungsten sinters at 1,800 °C [13]. In the samples with lower percentages of W, the ball milling process causes large, soft Cu particles to deform and encapsulate the small, hard W particles. However, when less copper is used, it is not as likely that the W will be coated with Cu meaning that the W particles will have to sinter directly which is much more unlikely at low temperatures. Figure 4 shows optical micrographs which indicate that the W particles are evenly distributed throughout the Cu matrix and that small clusters of W are visible in the Cu matrix for the samples with lower weight percentage of W. Figure 5a shows the corresponding SEM images of Cu–W sample from Fig. 4a which further confirmed the agglomeration of W particles, as well as a small amount of porosity (indicated by the arrow) that could be due to incomplete densification or a particle that may have been removed during sample preparation process. Figure 5b is an SEM image of sample Fig. 4c that shows the uniform distribution of W particles and demonstrated fully dense sintered sample, i.e., no porosity was visible. Figure 6 shows optical micrographs of the Cu–WC system which, again, show that the WC particles are evenly distributed in the Cu matrix.

To reach the maximum density, it was important to determine optimal process parameters of each composition. Figure 7 shows that higher sintering temperatures improve final density. During sintering at 1,000 °C, sintered samples exhibited melting of copper. As a result, most of the sintering was done at 975 °C. To push the envelope, one

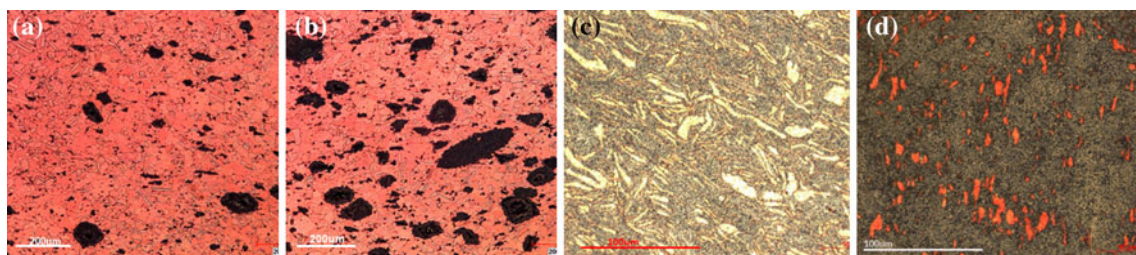


**Fig. 4** Optical images showing microstructures of Cu–W composites **a** 10 wt%, **b** 20 wt%, **c** 50 wt%, and **d** 70 wt% sintered at 975 °C and pressures ranging from **a** 36 MPa, **b** 36 MPa, **c** 45 MPa, and **d** 75 MPa. The darker regions in all of the images represent tungsten

**Fig. 5** SEM images of Cu–W  
**a** 10 wt% W showing agglomeration of W and  
**b** 50 wt% W showing uniform distribution of W, sintered at 975 °C at 36 and 45 MPa, respectively

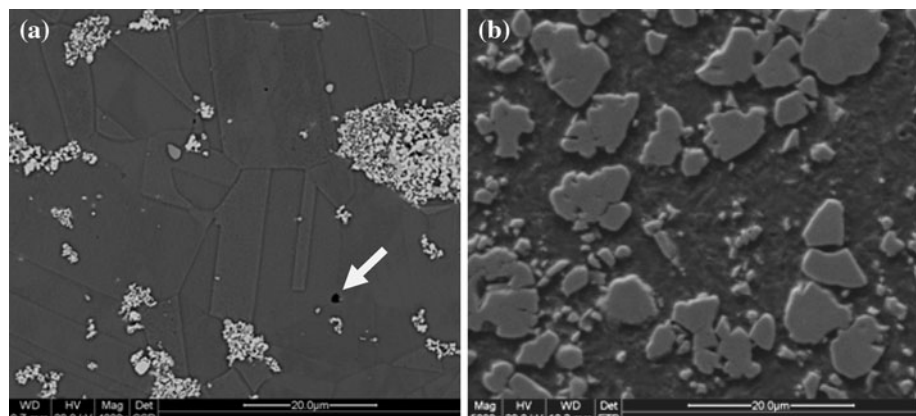
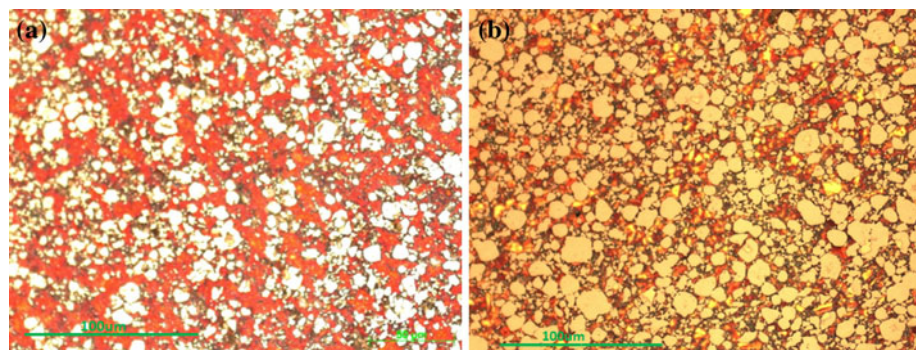


**Fig. 6** Optical images showing the microstructure of **a** Cu–50 wt% WC and **b** Cu–70 wt% WC for samples sintered at 975 °C, at 55 MPa (**a**) and 75 MPa (**b**)



sample made with 70 wt% WC was sintered at 990 °C and resulted in almost a 2% increase in density from 97% to almost 99%. This effect can be seen in Fig. 3.

Pressure and heating rate were also explored as possibly having an effect in the final density of the product. As expected, higher pressure led to an increase in the final density of the sample. This was observed in both Cu–70 wt% W and Cu–70 wt% WC. This is shown in Fig. 8. Higher applied pressure increases particle rearrangement (which can lead to greater neck formation), hot deformation, and also increases the driving force for sintering. This ultimately leads to higher density in the final sample.

The heating rate was varied from 25 to 100 °C/min and showed no effect on the final density of the sample. This result was expected and is in agreement with previous results of nano-crystalline Cu [14]. While heating rate does

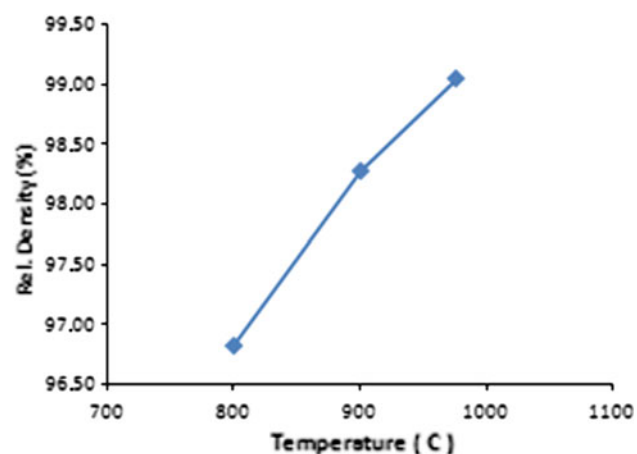


**Fig. 7** Density versus temperature data for Cu–10 wt% W shows the dependence of density on sintering temperature at 36 MPa

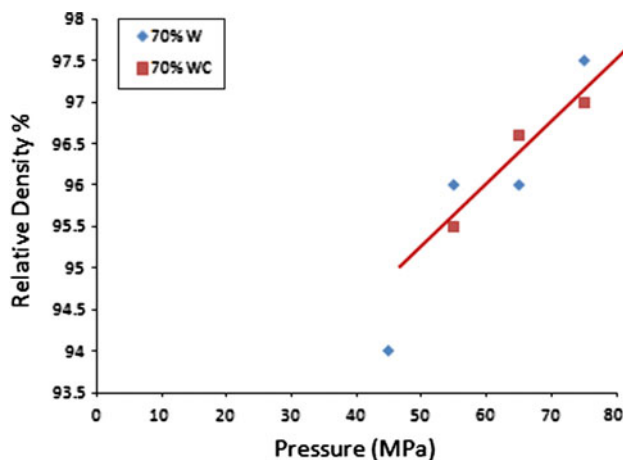


**Fig. 8** Effect of pressure on the final density of Cu–70 wt% W or WC sintered at 975 °C for 20 min

not affect density, it would be expected to reduce particle coarsening because the diffusion mechanisms that enable grain growth are much more active at higher temperatures. Higher heating rates would reduce the total time that the particles would spend at elevated temperatures. Particle coarsening reduces the driving force for sintering. Following from this, it would be expected that a higher heating rate would increase the final density. In this experiment, the samples were H<sub>2</sub> treated for 20–60 min at 700 °C. At this temperature, significant powder coarsening could occur and overcome the benefit of high heating rate. This explains the lack of effect of heating rate on final density. Figure 9 shows the effect of heating rate on the final density.

Figure 10 shows the value of the CTE for each of the different compositions of Cu–W and Cu–WC. As expected, adding more W or WC in the composite decreases the overall CTE of the composite. Small additions of W might not affect the composite's CTE since the W clusters are required to compensate for the Cu phase's expansion. Figure 10 shows that the CTE of the composite can be

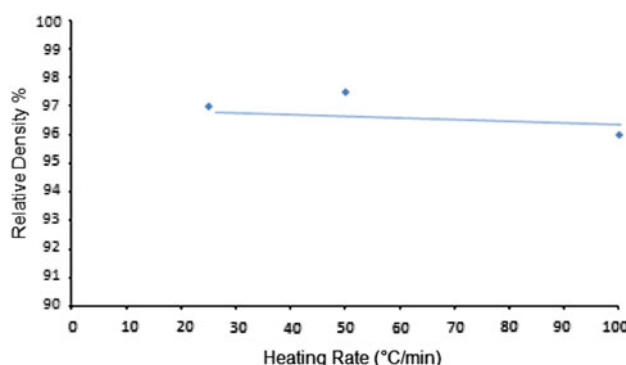


**Fig. 9** Effect of heating rate on sintered density for Cu–70 wt% W at 975 °C and 65 MPa

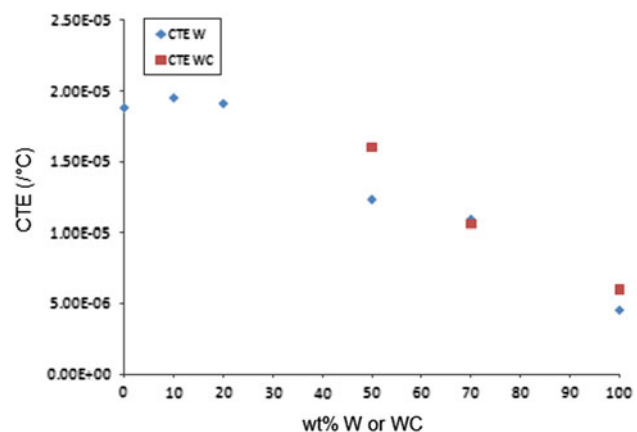


**Fig. 10** CTE measurements for the Cu–W and Cu–WC system

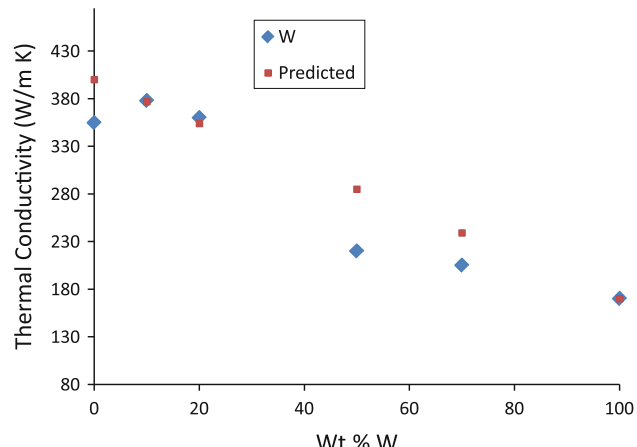
engineered by changing the amount of tungsten in the system.

Figure 11 shows the thermal conductivity values of Cu samples with varying amounts of W added as well as the predicted value for calculated using linear extrapolation. The predicted value was calculated using a linear interpolation method. The predicted value is given by the Eq. 7:

$$(\%W)xk_W + (1 - \%W)xk_{Cu}, \quad (7)$$

where  $k$  is the thermal conductivity. As expected, increasing the amount of W reduces the overall thermal conductivity of the composite. It should be noted that the value of the pure copper sample was measured using a commercial oxygen free Cu sample (not fabricated using the FAST process) as a baseline material. The value for pure W is the given book value, and was not directly measured [15].

The densities reported in this article are among the highest values reported for this the Cu–W system. The difference between the current work and previous works is that a one step, solid state process is used to engineer



**Fig. 11** Thermal conductivity and predicted value of selected Cu–W samples

Cu–W composites with varying ratios of each constituent. The value of CTE for 70 wt% W is in agreement with previous work [4]. The thermal conductivity value for 50 wt% W is also in agreement with previously reported values [9]. Our study also demonstrated that a heat sink can be fabricated with a functional graded composition that is engineered in such a way that the critical portion of the heat sink can have a low CTE followed copper that has a high thermal conductivity.

## Conclusion

High density samples of Cu–W and Cu–WC were created using the FAST method. Densities of above 97% were reported for all compositions, and 99% were reported for all cases except when the major component in the system was tungsten. It was shown that the FAST method can quickly produce high quality Cu–W composite materials that can be engineered to specific CTE and thermal conductivity needs by varying the amount of tungsten that is added to the system. The CTE ranged from  $20 \times 10^{-6}/^{\circ}\text{C}$  to  $10 \times 10^{-6}/^{\circ}\text{C}$  with increasing amounts of W. The closest CTE value of the composite to that of silicon composite was  $10 \times 10^{-6}/^{\circ}\text{C}$ . The corresponding thermal conductivity of this composite was 205 W/m K. This is double the value of silicon. It was shown that both increased sintering temperature and pressure positively impact the final density of the sample while heating rate did not have an effect on the final density. The FAST method is effective way to produce Cu–W composite and

other composite materials for use in heat sink as well as other applications.

## References

1. Chu RC, Simons RE, Ellsworth MJ, Schmidt RR, Cozzolino V (2004) IEEE Trans Device Mater Reliab 4:568
2. German RM, Suri P, Park SJ (2009) J Mater Sci 44:1. doi: [10.1007/s10853-008-3008-0](https://doi.org/10.1007/s10853-008-3008-0)
3. Smid I, Akiba M, Vieider G, Plochl L (1998) J Nucl Mater (Neth) 258–263:160
4. Ibrahim A, Abdallah M, Mostafa S, Hegazy A (2009) Mater Des 30:1398
5. Rosinski M, Fortuna E, Michalski A, Pakiela Z, Kurzydlowski KJ (2007) Fusion Eng Des 82:2621
6. Zhang Q, Shi X, Yang H, Duan X (2008) J Wuhan Univ Technol Mater Sci Ed 23:399
7. Kim B, Hiraga K, Morita K, Yoshida H (2009) J Eur Ceram Soc 29:323
8. Zhang Z, Wang F, Wang L, Li S (2008) Mater Sci Eng A 476:201
9. Lee S, Noh J-W, Johnson JL, Park SJ, German RM (2006) In: Advances in powder metallurgy and particulate materials—2006. Metal Powder Industries Federation, Princeton
10. Olevsky EA, Kandukuri S, Froyen L (2007) J Appl Phys 102:114913
11. Groza JR, Zavalangos A (2000) Mater Sci Eng A (Switz) 287:171
12. Chiba H, Ogushi T, Nakajima H, Torii K, Tomimura T, Ono F (2008) J Appl Phys 103:01315-1
13. Kecske LJ, Cho KC, Dowding RJ, Schuster BE, Valiev RZ, Wei Q (2007) Mater Sci Eng A 467:33
14. Zhang ZH, Wang FC, Lee SK, Liu Y, Cheng JW, Liang Y (2009) Mater Sci Eng A 523:134
15. German RM, Hens KF, Johnson JL (1994) Int J Powder Metall 30:205